The Origin of the Universe, Part 1: Toryces

Vladimir B. Ginzburg
IRMC, Inc., Helicola Press, 612 Driftwood Drive, Pittsburgh, PA 15238
e-mail: helicola@aol.com

Toryces are polarized prime elements of nature forming elementary matter particles. Polarization of toryces is accomplished by the inversion of their spacetimes. Polarized states of toryces are sustained by their spiral motions in accordance with a newly-discovered universal law of motion. Based on three fundamental spacetime equations, the toryces exist in several topological forms in which the amplitudes of their polarized properties vary from infinity to infinility (the inverse of infinity). This allows the properly-matched polarized toryces to form an entire range of known elementary particles. Formation of stable elementary mass particles follows a newly-discovered universal conservation law.

1. Fundamental Spacetime Equations of Toryx

According to the 3-Dimensional Spiral String Theory (3D-SST) [1-16], toryx is a spacetime spiral string element containing a circular leading string with the radius r_1 and a toroidal trailing string with the radius r_2 (Fig. 1).

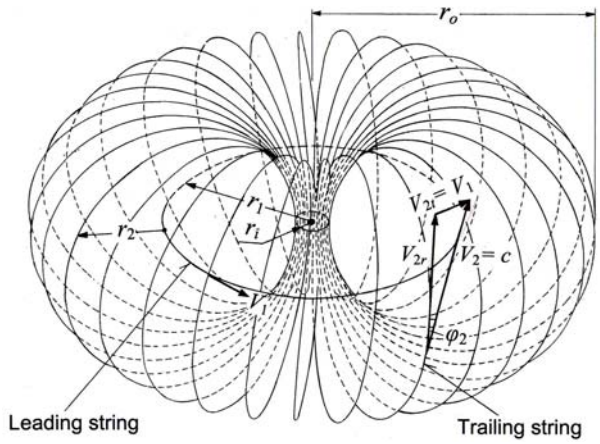

Fig. 1. Spacetime parameters of toryx

The other spacetime parameters of the toryx shown in Fig. 1 are:

r_o = outer toryx radius
r_i = radius of real inversion string
φ_2 = steepness angle of trailing string
V_1 = velocity of leading string
V_{2r} = rotational velocity of trailing string
V_{2t} = translational velocity of trailing string
V_2 = spiral velocity of trailing string

When $r_1 = r_i$, toryx reduces to the *real inversion string*. This is a circular string (Fig. 2) propagating with the velocity of light c. The toryx spacetime parameters are based on three fundamental equations shown in Table 1.

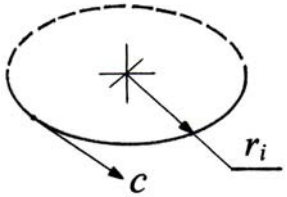

Fig. 2. The real inversion string

Length of one winding of trailing string	$L_2 = L_1$	(1)
Inversion radius of real inversion string	$r_i = r_1 - r_2 = const.$	(2)
Spiral velocity of trailing string	$V_2 = \sqrt{V_{2r}^2 + V_{2t}^2} = c = const.$	(3)

Table 1. Toryx fundamental spacetime equations

Let us summarize the meaning of the toryx fundamental equations (1) – (3).

- Eq. (1) stipulates that the length of one winding of trailing string L_2 is equal to the length of one winding of leading string L_1.
- Eq. (2) establishes that the difference between radii of leading string r_1 and trailing string r_2 is equal to the radius of real inversion string r_i that is assumed to be constant.
- Eq. (3) assigns the value for the spiral velocity of trailing string V_2 to be equal to the velocity of light in the vacuum c that is constant. It is very important to notice that Eq. (3) sets no limits on the values of the two components of the spiral velocity V_2: the rotational velocity V_{2r} and the translational velocity V_{2t}. Any one of them can be superluminal making the other one imaginary to satisfy Equation (3).

Since the radius of real inversion string r_i and the spiral velocity of trailing string V_2 are constant, we can identify two more parameters of the real inversion string that are also constant. They are the frequency f_i and the cycle time t_i that are expressed by the equations.

$$f_i = \frac{c}{2\pi r_i} = const. \quad (4)$$

$$t_i = \frac{2\pi r_i}{c} = const. \quad (5)$$

Therefore, we can express the toryx spacetime parameters in relative terms in respect to the four constant parameters: r_i, f_i, t_i, and c.

2. Derivative Spacetime Equations of Toryx

Tables 2 and 3 show derivative equations for the relative spacetime parameters of the toryx leading and trailing strings.

These equations are derived based on the toryx fundamental spacetime equations (1), (2) and (3).

Parameter	Equation	
Relative length	$l_1 = \frac{L_1}{2\pi r_i} = b_1$	(6)
Relative radius	$b_1 = \frac{r_1}{r_i}$	(7)
Relative velocity	$\beta_1 = \frac{V_1}{c} = \pm\frac{\sqrt{2b_1 - 1}}{b_1}$	(8)
Relative frequency	$\delta_1 = \frac{f_1}{f_i} = \frac{\sqrt{2b_1 - 1}}{b_1^2} \pm$	(9)
Relative cycle time	$\tau_1 = \frac{t_1}{t_i} = \pm\frac{b_1^2}{\sqrt{2b_1 - 1}}$	(10)

Table 2. Relative spacetime parameters of leading string as a function of the relative radius of leading string b_1.

Parameter	Equation	
Relative radius	$b_2 = \frac{r_2}{r_i} = b_1 - 1$	(11)
The number of windings	$w_2 = \pm\frac{b_1}{\sqrt{2b_1 - 1}}$	(12)
Relative volume	$u_2 = \frac{U_2}{2\pi^2 r_i^3} = b_1(b_1 - 1)^2$	(13)
Relative wavelength	$\eta_2 = \frac{\lambda_2}{2\pi r_i} = \pm\sqrt{2b_1 - 1}$	(14)
Relative spiral velocity	$\beta_2 = \frac{V_2}{c} = \sqrt{\beta_{2r}^2 + \beta_{2t}^2} = 1$	(15)
Relative rotational velocity	$\beta_{2r} = \frac{V_{2r}}{c} = \frac{b_1 - 1}{b_1}$	(16)
Relative translational velocity	$\beta_{2t} = \frac{V_{2t}}{c} = \pm\frac{\sqrt{2b_1 - 1}}{b_1}$	(17)
Steepness angle	$\cos u(\phi_2) = \frac{b_1 - 1}{b_1}$	(18)
Relative frequency	$\delta_2 = \frac{f_2}{f_i} = \frac{1}{b_1}$	(19)
Relative cycle time	$\tau_2 = \frac{t_2}{t_i} = b_1$	(20)

Table 3. Relative spacetime parameters of trailing string at a middle point as a function of the relative radius of leading string b_1.

Below is the nomenclature for the parameters of the derived equations.

l_1 = relative length of leading string
l_2 = relative length of trailing string
b_1 = relative radius of leading string
b_2 = relative radius of trailing string
b_o = toryx relative outer radius
β_1 = relative velocity of leading string
β_2 = relative spiral velocity of trailing string
β_{2r} = relative rotational velocity of trailing string
β_{2t} = relative translational velocity of trailing string
f_1 = frequency of leading string
f_2 = frequency of trailing string
δ_1 = relative frequency of leading string
δ_2 = relative frequency of trailing string
t_1 = cycle time of leading string
t_2 = cycle time of trailing string
τ_1 = relative cycle time of leading string
τ_2 = relative cycle time of trailing string
w_2 = the number of windings of trailing string
λ_2 = wavelength of trailing string
η_2 = relative wavelength of trailing string
U_2 = volume of trailing string
u_2 = relative volume of trailing string

The toryx relative outer radii b_o is equal to:

$$b_o = 2b_1 - 1 \tag{21}$$

Inner velocities *at point a′*	**Outer velocities** *at point a″*
$\beta_{2t}^{in} = \frac{\sqrt{2b_1 - 1}}{b_1^2}$ (22)	$\beta_{2t}^{out} = \frac{(2b_1 - 1)^{3/2}}{b_1^2}$ (24)
$\beta_{2r}^{in} = \frac{\sqrt{b_1^4 - 2b_1 + 1}}{b_1^2}$ (23)	$\beta_{2r}^{out} = \frac{\sqrt{b_1^4 - (2b_1 - 1)^3}}{b_1^2}$ (25)
$\beta_{2t}^{in} > 1$ $0.544 < b_1 < 1.0$	$\beta_{2t}^{out} > 1$ $1.0 < b_1 < 6.222$

Table 4. Relative peripheral velocities of trailing string

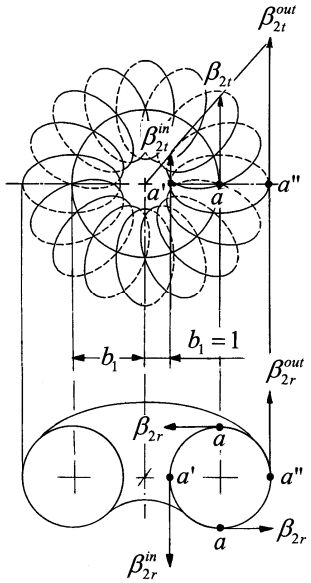

Fig. 3. Peripheral velocities of trailing string

To maintain integrity of the toryx, the translational velocity of its trailing string β_{2t} must increase proportionally with the distance from the toryx center as illustrated in Fig. 3. Table 4 shows the equations for the peripheral velocities of the toryx trailing

strings. It also shows the ranges of the relative radii of leading string b_1 within which either the relative inner translation velocity β_{2t}^{in} or the relative outer translational velocity β_{2t}^{out} are greater than 1, meaning that their absolute values exceed the velocity of light *c*, or *superluminal*.

3. Three Main Features of the Toryx Math

The three main features of the toryx math include:

- New interpretation of zero
- Modification of trigonometric functions
- New presentation of a number line.

3.1 New Interpretation of Zero

Conventionally, zero is considered as one of the integers. 3D-SST replaces the conventional zero with a so-called *infinility* that means "infinite nil," or "infinite zero." The theory defines infinility as an inverse of infinity. Most of us learned about the infinity in school. Unlike the finite quantities such as 1, 2, 100, 2500, etc., an infinite quantity cannot be completely counted or measured. So, the infinity is *larger* than any finite quantity. We can arrive to the infinity, for instance, by multiplying a finite quantity 1 by 10, 100, 1000, etc.. The infinity can be either real positive ($+\infty$) or real negative ($-\infty$). It can also be either imaginary positive ($+\infty i$) or imaginary negative ($-\infty i$).

Similarly to the infinity, the infinility cannot be completely counted or measured. But, oppositely to the infinity, the infinility is *smaller* than any finite quantity. We can logically arrive to the infinility, for instance, by dividing 1 by 10, 100, 1000, etc.. Similarly to the infinity, the infinility can be either real positive (+0) or real negative (-0). It can also be either imaginary positive (+0*i*) or imaginary negative (-0*i*).

The introduction of infinility changes our view of finite quantities. Since the difference between any quantities cannot any longer be equal to zero, the quantities that are precisely equal to one another do not exist. Consequently, there are no any finite quantities. We can only approach a quantity *X* infinitely close from larger and smaller values of this quantity.

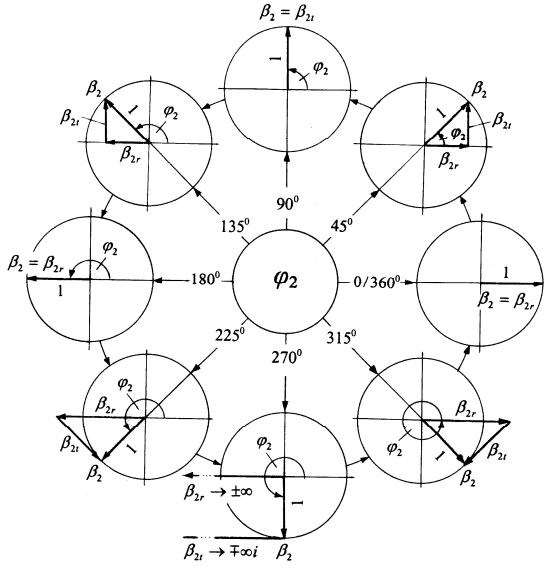

Fig. 4. The triangle of velocities of the toryx trailing string

3.2 Modification of Trigonometric Functions

3D-SST utilizes a so-called *universal trigonometry* (Fig. 4) that is partially different than a conventional trigonometry. We added a letter *u* to the names of the universal trigonometric functions to separate them from the classical ones.

Fig. 4 shows the triangle of velocities the toryx trailing string utilizing the universal trigonometry. The toryx triangle of velocities is made up of three vectors representing the relative velocities of trailing string: the relative rotational velocity β_{2r}, the relative translational velocity β_{2t} and the relative spiral velocity β_2.

As follows from Eq. (18), within the range of the steepness angle of trailing string φ_2 from 0 to π, the universal trigonometric functions are the same as those used in a conventional trigonometry. Within the range of φ_2 from π to 2π, the classical trigonometric functions are constructed based on a mirror image of those function within the range φ_2 from 0 to π.

The universal trigonometric functions within the range of φ_2 from □ to 2π are different than the classical functions, and they are related to one another by the equations shown in Table 5 and Eq. (26).

Universal	**Conventional**	
$(0 < \varphi_2 < 2\pi)$	$(0 < \varphi_2 < \pi)$	$(\pi < \varphi_2 < 2\pi)$
$\cos u(\varphi_2)$	$\cos(\varphi_2)$	$\cos^{-1}(\varphi_2)$
$\sin u(\varphi_2)$	$\sin(\varphi_2)$	$i\tan(\varphi_2)$
$\tan u(\varphi_2)$	$\tan(\varphi_2)$	$i\tan(\varphi_2)\cos^{-1}(\varphi_2)$

Table 5. Relationship between universal and conventional trigonometric functions

$$\varphi_2 = \arccos\left(\frac{b_1 - 1}{b_1}\right) \quad (0 < \varphi_2 < \pi) \tag{26a}$$

$$\varphi_2 = 2\pi - \arccos\left(\frac{b_1}{b_1 - 1}\right) \quad (\pi < \varphi_2 < 2\pi) \tag{26b}$$

3.3 New Presentation of a Number Line

As shown in Figure 5, a conventional number line presents the numbers *b* extending along a straight line from zero to the right towards the positive infinity ($+\infty$) and to the left towards the negative infinity ($-\infty$). Notably, the zero is treated in this number line as an integer and the distance between zero and one is the same as the distances between any other adjacent numbers.

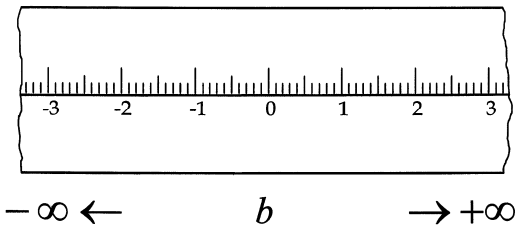

Fig. 5. Conventional number line

3D-SST utilizes two kinds of universal number lines in which the numbers represent the two polarization parameters of a toryx, the *toryx vorticity* $\tilde{V}$ (Fig. 6) and the *toryx reality* $\tilde{R}$ (Fig. 7).

Both lines are circular and the angular positions of the toryx parameters are expressed there as a function of the toryx steepness angle φ_2.

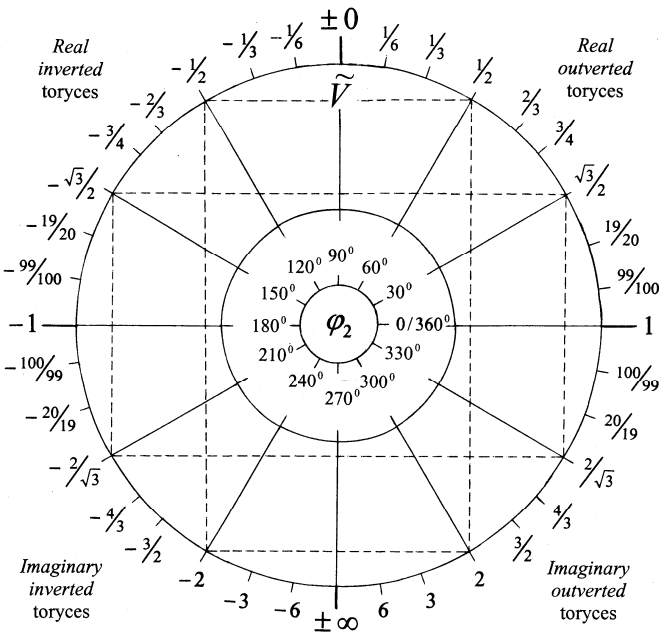

Fig. 6. Universal number line based on the toryx vorticity $\tilde{V}$.

The toryx vorticity $\tilde{V}$ is equal to the ratio of the toryx trailing and leading strings, and is expressed by the equation:

$$\gamma = \frac{r_2}{r_1} = \frac{b_1 - 1}{b_1} = \beta_{2r} = \cos u(\varphi_2) \qquad (27)$$

The $\tilde{V}$ universal number line is divided into four distinct quadrants:

- **Top right quadrant** $(+0 < \varphi_2 < \pi/2)$. Within this quadrant $\tilde{V}$ decreases from +1 to +0.
- **Top left quadrant** $(\pi/2 < \varphi_2 < \pi)$. Within this quadrant $\tilde{V}$ decreases from -0 to -1.
- **Bottom left quadrant** $(\pi < \varphi_2 < 3\pi/2)$. Within this quadrant $\tilde{V}$ decreases from -1 to -∞.
- **Bottom right quadrant** $(3\pi/2 < \varphi_2 < 2\pi)$. Within this quadrant $\tilde{V}$ decreases from +∞ to +1.

In this line the infinilities of opposite signs (± 0) merge at the borderline between the top quadrants, while the infinities of opposite signs ($\pm\infty$) merge at the borderline between the bottom quadrants. The top quadrants are called the *infinility domain*, and the bottom quadrants the *infinity domain*. Notably, both domains occupy the same space on the number line.

There is a *unique symmetry* between the values of $\tilde{V}$ that belong to four different quadrants of the $\tilde{V}$ universal number line. The character of symmetries is different in horizontal and vertical directions of the number line. In the horizontal direction, the absolute values of $\tilde{V}$ in the top right and left quadrants are same, but they have opposite signs. The same is true for the values of $\tilde{V}$ in the bottom right and left quadrants. In the vertical direction, the values of $\tilde{V}$ in the left top quadrant are the inverse of the values $\tilde{V}$ of the left bottom quadrant. The same is true for these values in the right top and bottom quadrants.

The toryx reality $\tilde{R}$ is equal to the relative wavelength of the toryx trailing string, and is expressed by the equation:

$$\tilde{R} = \eta_2 = \pm\sqrt{2b_1 - 1} = \pm\sqrt{\frac{1+\cos u(\varphi_2)}{1-\cos u(\varphi_2)}} \qquad (28)$$

The $\tilde{R}$ universal number line is similar to the $\tilde{V}$ universal number line in two ways. Firstly, both of them are divided into four similar distinct quadrants. Secondly, they both have a unique symmetry between the values of the numbers that belong to the four different quadrants. There is, however, a substantial difference between these two lines. In the $\tilde{V}$ universal number line all numbers are real, but in the $\tilde{R}$ universal number line the real numbers reside only in the top two quadrants, while the bottom two quadrants are occupied by the imaginary numbers. Consequently, the $\tilde{R}$ number line provides for a merge of two extremities: the real and imaginary infinilities ($+\infty/-\infty i$) and the real and imaginary infinities ($+\infty/-\infty i$).

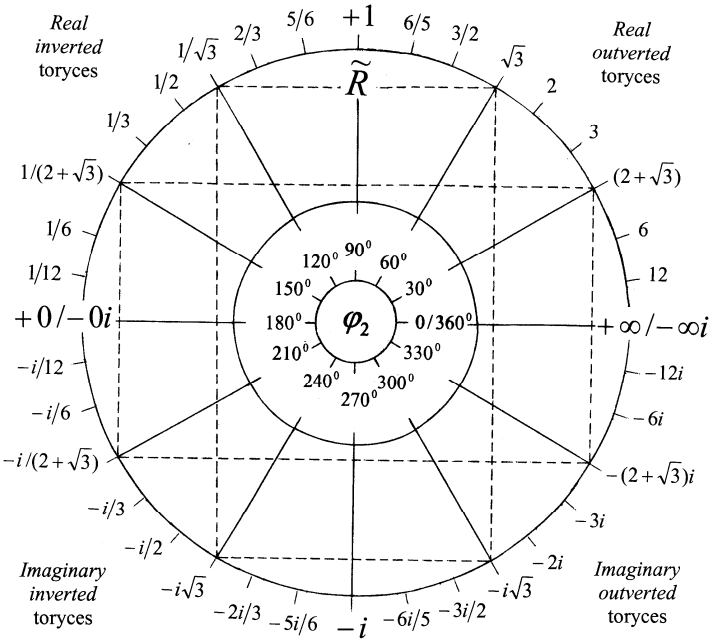

Fig. 7. Universal number line based on the toryx reality $\tilde{R}$.

In both universal number lines, each quadrant corresponds to a different kind of toryces. The main classification of toryces is based on two types of their polarization, reality and vorticity.

Reality-polarized toryces. These toryces are divided into *real* and *imaginary*. The real toryces occupy the two top quadrants of both universal number lines. All their spacetime parameters for the middle of the toryx trailing string are expressed with the real numbers. The imaginary toryces occupy the two bottom quadrants of both universal number lines. Some of their spacetime parameters for the middle of the toryx trailing string are expressed with the imaginary numbers.

Vorticity-polarized toryces. Both real and imaginary toryces can be either *outverted* or *inverted*. Trailing strings of the outverted toryces are wound outside the real inversion string, while the trailing strings of the inverted toryces are wound inside the real inversion string.

4. Trends of Toryx Spacetime Parameters

It is most convenient to observe the trends of the toryx spacetime parameters for different kinds of toryces when these parameters are expressed as a function of the steepness angle of trailing string φ_2 as shown in Figs. 8 – 16. Notably, all toryx spacetime parameters approach either the infinility (± 0) or infinity ($\pm\infty$) when the steepness angles of trailing string φ_2 are equal to 0, 90^0, 180^0, 270^0 and 360^0.

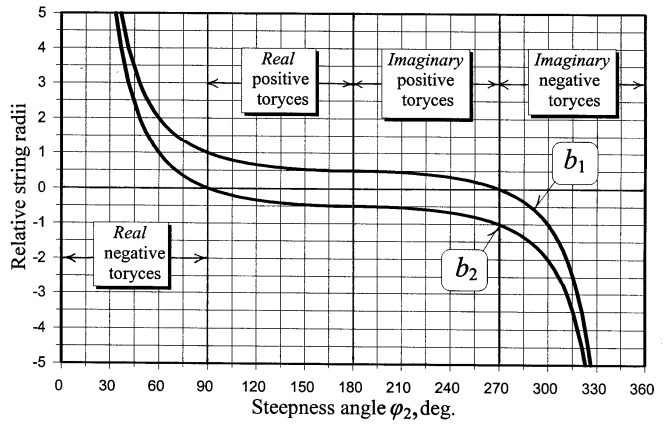

Fig. 8. The trends of the relative radii of leading string b_1 and trailing string b_2 as a function of the steepness angle of trailing string φ_2

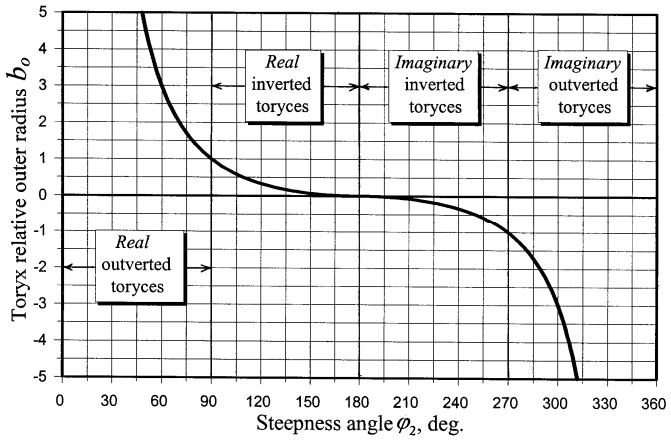

Fig. 9. The trend of the toryx relative outer radius b_o as a function of the steepness angle of trailing string φ_2

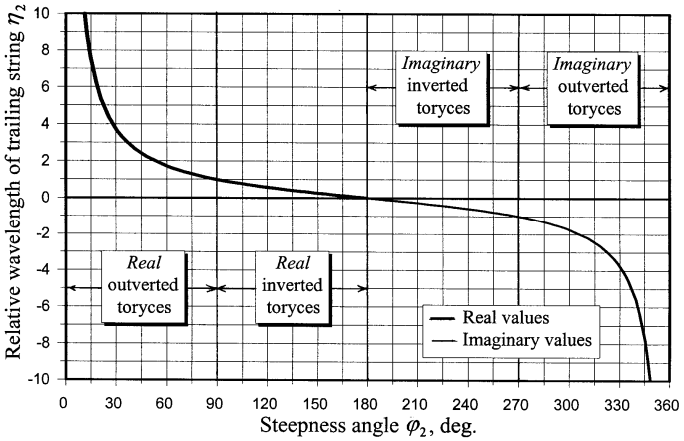

Fig. 10. The trend of the relative wavelength of trailing string η_2 as a function of the steepness angle of trailing string φ_2

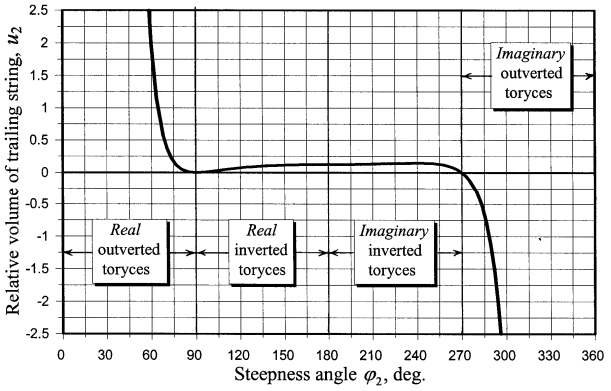

Fig. 11. The trend of the relative volume of trailing string u_2 as a function of the steepness angle of trailing string φ_2

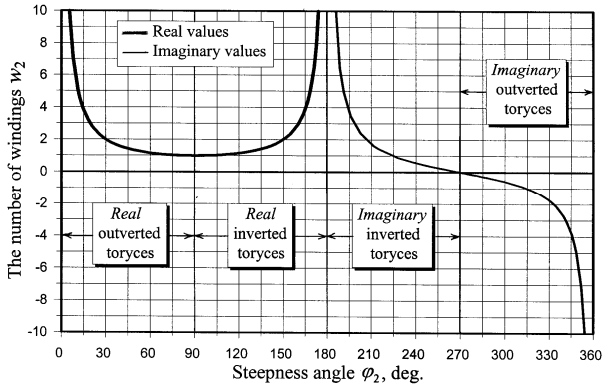

Fig. 12. The trend of the number of windings of trailing string w_2 as a function of the steepness angle of trailing string φ_2

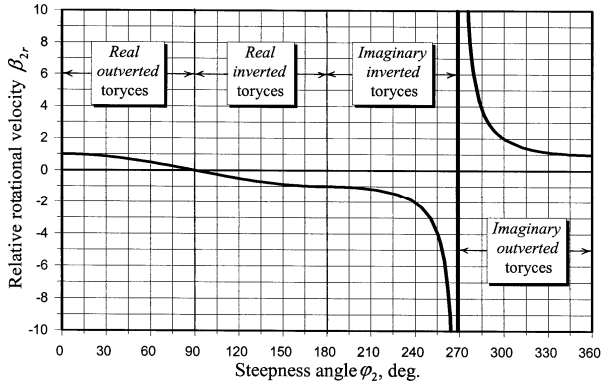

Fig. 13. The trend of the relative rotational velocity of trailing string β_{2r} as a function of the steepness angle of trailing string φ_2

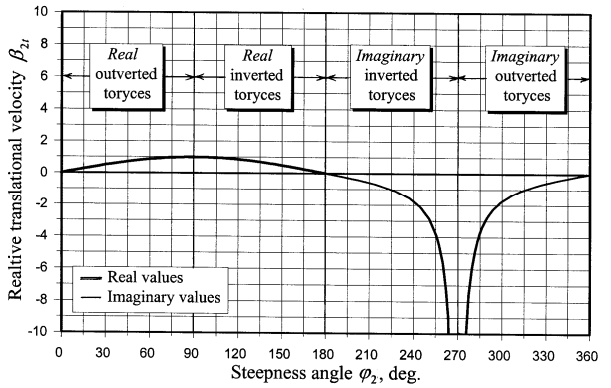

Fig. 14. The trend of the relative translational velocity of trailing string β_{2t} as a function of the steepness angle of trailing string φ_2

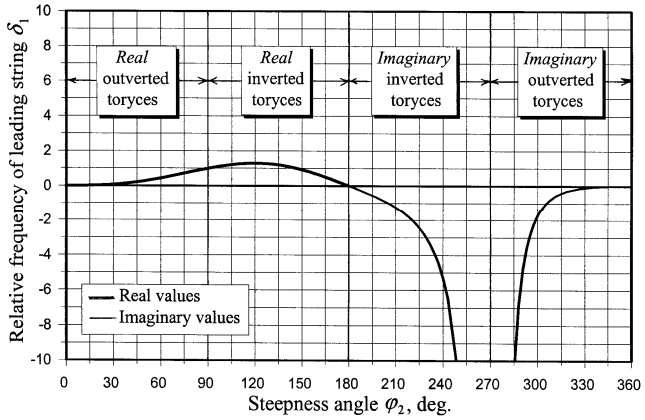

Fig. 15. The trend of the relative frequency of leading string δ_1 as a function of the steepness angle of trailing string φ_2

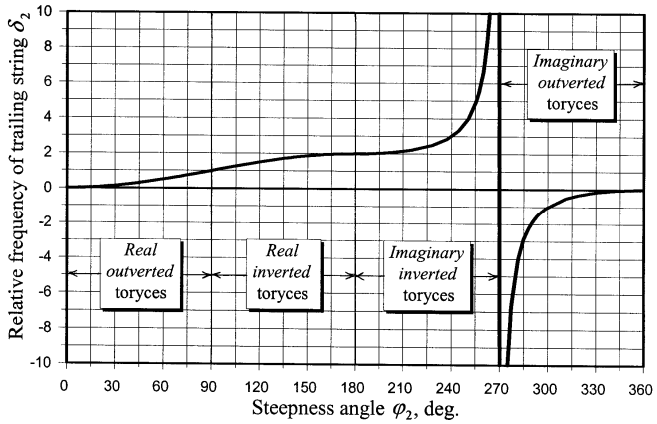

Fig. 16. The trend of the relative frequency of trailing string δ_2 as a function of the steepness angle of trailing string φ_2

5. Metamorphoses of Toryx Topology

The metamorphoses of the toryx topology involve the inversion of its spacetime. One of the mostly known topological shapes that involves the inversion is the *Möbius strip* originally invented by the German mathematician Johann Listing in 1861, and thoroughly explained several years later by the German mathematician and astronomer Ferdinand Möbius (1790-1868).

Take a piece of paper, rotate one end through 180 degrees and connect the ends together (Fig. 17). An ant walking on the inside part of the Möbius strip will eventually end up on the outer part of the strip. Thus, the Möbius strip makes a smooth transition from the outverted black surface to the inverted white surface turned inside out.

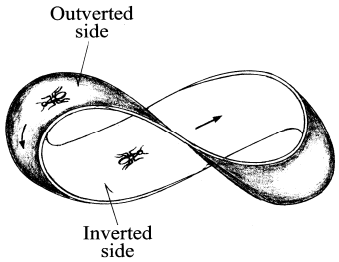

Fig. 17. The Möbius strip

The inversion of the toryx spacetime involves the inversion of its leading and trailing strings. Let us consider first the inversion of an outverted trailing string wound outside the real inversion string with the radius r_i as the radius of leading string r_1 decreases (Fig. 18). Initially, the radius of trailing string is positive ($r_2 > 0$) and its external color is assumed to be black, while its internal color is white. As the relative radius of leading string r_1 decreases, but remains to be greater than r_i, the trailing string simply becomes slimmer, and the number of its windings w_2 decreases.

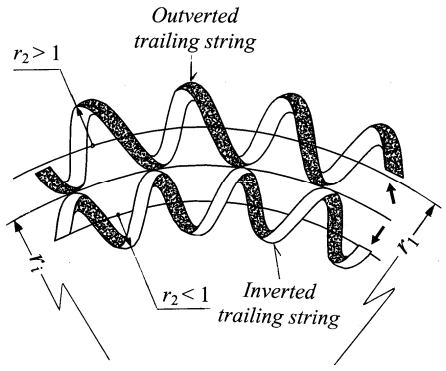

Fig. 18. Inversion of trailing string

When r_1 becomes infinitesimally close to r_i, a real transformation of a toryx shape occurs. The trailing string reduces to a circle that appears in Figure 18 as a colorless edge of a ribbon. In fact, when $r_1 = r_i$, the trailing string merges with the leading string. After r_1 becomes smaller than r_i, the sign of the radius r_2 changes from positive to negative and the trailing string turns inside out, or becomes inverted. Consequently, its external color becomes white and its spin reverses.

The transformation of the toryx leading string proceeds in a similar manner (Fig. 19). When the radius of leading string is positive ($r_1 > 0$), the leading string is outverted, and its external color is assumed to be black, while its internal color is white. After r_1 decreases and becomes infinitesimally close to the positive infinility (+0), the leading string reduces to a point, making the string both dimensionless and colorless. At this point, the positive infinility (+0) transforms into the negative infinility (-). Consequently, the leading string turns inside out, or becomes inverted, and its external color changes to white.

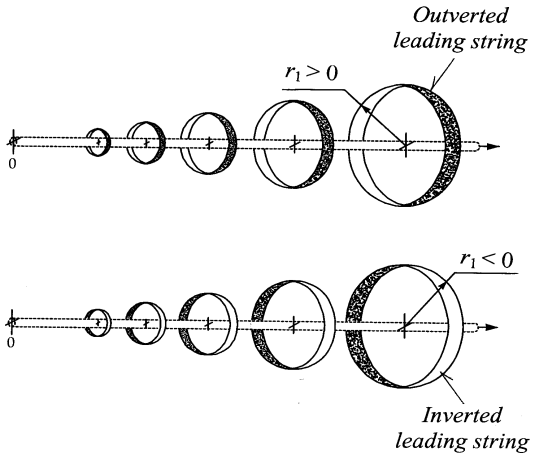

Fig. 19. Inversion of leading string

Based on the equations for the spacetime properties of a toryx shown in Tables 2 and 3, we can visualize unique spacetime transformations of the toryx shown in Figures 20-23.

Real outverted toryces. These toryces are located at the top right quadrant of the universal number lines shown in Figs. 6 and 7 $(+0 < \varphi_2 < \pi/2)$, $(+\infty > b_1 > 1)$. The transformations of their topology are shown in Fig. 20:

- At the beginning of this range the relative radius of leading strings b_1 approaches real positive infinity $(+\infty)$. The same is true for the relative radius of trailing string b_2 and the number of windings w_2. Consequently, the trailing string appears as two infinitely long straight lines called the *outverted inversion string*. The string is perpendicular to a circle with the radius $b_1 = 1$.
- As φ_2 increases and b_1 decreases, the relative radius of trailing string b_2 decreases, and the number of windings w_2 decreases. Consequently, the trailing string appears like a toroidal spiral with diminishing dimensions.
- At the end of the range, the relative radius of trailing string b_2 approaches the real positive infinility (+0) and the number of windings reduces to one ($w_2 \rightarrow 1$). Consequently, the trailing string merges with the leading string and the toryx reduces to a circle with the relative radius $b_1 \rightarrow 1$, representing the real inversion string.

Real inverted toryces. These toryces are located at the top left quadrant of the universal number lines shown in Figs. 6 and 7 $(\pi/2 < \varphi_2 < \pi)$, $(1 > b_1 > 1/2)$. The transformations of their topology are shown in Fig. 21. The main transformations of the topology of these toryces are:

- Within this range the toryx is still real, but its trailing string is inverted, or turned inside out, so its windings are now located inside the real inversion string.
- As the relative radius of leading string b_1 becomes less than 1 and continues to decrease, both the negative value of the relative radius of trailing string b_2 and the number of windings w_2 increase.
- At the end of the range, when $b_1 \rightarrow 0.5$ and $b_2 \rightarrow$ -0.5, the inner parts of the toryx opposite windings began to touch one another and the toryx eye disappears. Consequently, the toryx reduces to the *inverted inversion string*. In the inverted inversion string, the number of windings w_2 approaches the real positive infinity (+∞).

Imaginary inverted toryces. These toryces are located at the bottom left quadrant of the universal number lines shown in Figs. 6 and 7 $(\pi < \varphi_2 < 3/2\,\pi)$, $(1/2 < b_1 < +0)$. The transformations of their topology are shown in Fig. 22. The main transformations of topology of these toryces are:

- At the beginning of this range, the number of windings w_2 approaches imaginary negative infinity (-∞i). As soon as the relative radius of leading string b_1 becomes less than 0.5, the opposite parts of windings of trailing string start to intersect with one another.
- As φ_2 increases and b_1 decreases, the negative value of the relative radius of trailing string b_2 increases and the imaginary number of windings w_2 decreases.
- At the end of the range, the relative radius of leading string b_1 approaches the real positive infinility (+0), the relative radius of trailing string b_2 approaches – 1, and the number of windings w_2 approaches the imaginary negative infinility (– 0i). Consequently, the toryx trailing string reduces to a circle called the *imaginary inversion string*. The imaginary inversion string is located in the plane perpendicular to the plane of the real inversion string shown in Figs. 20 and 21.

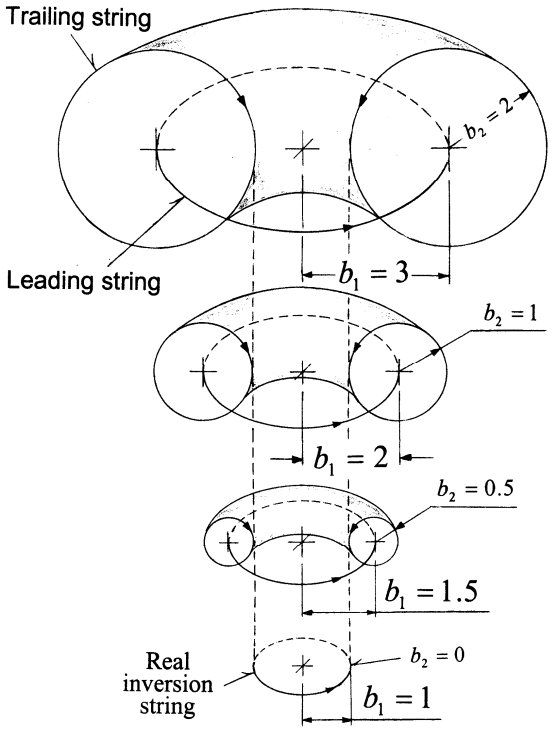

Fig. 20. Topology of a real outverted toryx $(0 < \varphi_2 < \pi/2)$, $(+\infty > b_1 > 1)$

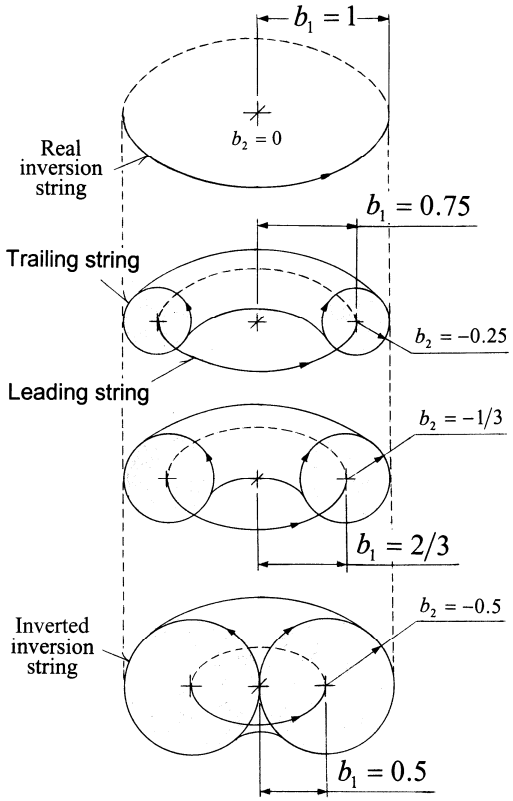

Fig. 21. Topology of a real inverted toryx $(\pi/2 < \varphi_2 < \pi)$, $(1 > b_1 > 1/2)$

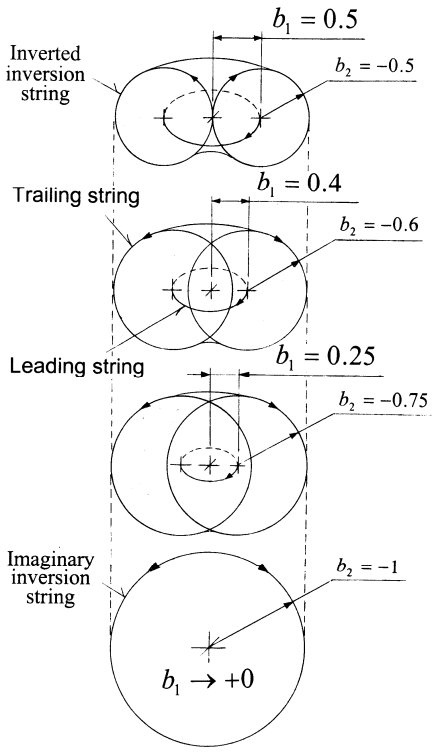

Fig. 22. Topology of an imaginary inverted toryx
$(\pi < \varphi_2 < {}^3\!/_2\,\pi)$, $({}^1\!/_2 > b_1 > +0)$

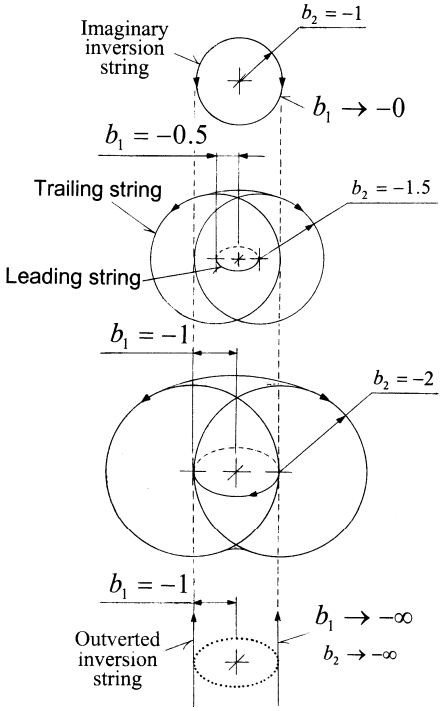

Fig. 23. Topology of an imaginary outverted toryx
$({}^3\!/_2\,\pi < \varphi_2 < 2\pi)$, $(-0 > b_1 > -\infty)$

Imaginary outverted toryces. These toryces are located at the bottom left quadrant of the universal number lines shown in Figs. 6 and 7 $({}^3\!/_2\,\pi < \varphi_2 < 2\pi)$, $(-0 < b_1 < -\infty)$. The transformations of their topology are shown in Fig. 23. The main transformations of topology of these toryces are:

- At the very beginning of the range the sign of the relative radius of leading string b_1 becomes negative and the leading string becomes inverted, or turned inside out. Consequently, the toryx appears as the imaginary inversion string in which the relative radius of leading string b_1 approaches the real negative infinility (-0), the relative radius of trailing string b_2 approaches – 1, while the number of windings w_2 approaches imaginary negative infinility (-0i).
- As the negative value of the relative radius of leading string b_1 increases, the negative values of the relative radius of trailing string b_2 also increase. Also increase is the imaginary negative number of windings w_2.
- At the end of the range, the relative radius of trailing string b_2 approaches the real negative infinity (-∞) and the number of windings w_2 approaches the imaginary negative infinity (-∞i). At this point, the toryx reduces to the *negative inversion string* that appears similar to the one shown in Figure 10, except for the directions of propagation of the strings that are opposite to one another.

Figure 24 shows the metamorphoses of the toryx topology in a circular diagram as a function of the steepness angle of trailing string φ_2.

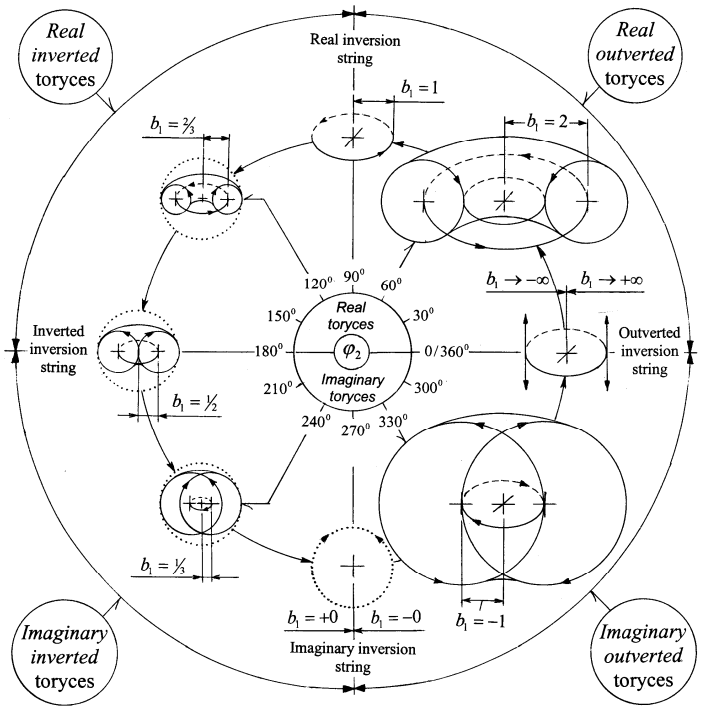

Fig. 24. Metamorphoses of the toryx topology as a function of the steepness angle of trailing string φ_2

6. Physical Properties of Toryces

6.1. Fundamental Physical Constants of Toryces

We will first express in physical terms the two spacetime constants: the radius of real inversion string r_i and the frequency of the real inversion string f_i. These constants correspond to the case when the effects of electric forces are negligibly small in comparison with the effects of gravity.

The radius of real inversion string r_i is given by the equation:

$$r_i = \frac{Ze_0^2}{8\pi\varepsilon_0 m_0 c^2} \tag{29}$$

The frequency of real inversion string f_i is equal to:

$$f_i = \frac{4\varepsilon_0 m_0 c^3}{Ze_0^2} \tag{30}$$

In Eqs. (29) and (30):

Z = atomic number
ε_0 = electric constant
e_0 = elementary charge
m_0 = rest mass of electron.

6.2. Toryx Charge, Mass and Energy

The toryx charge and mass are assumed to be a function of the toryx vorticity $\tilde{V}$, as shown in Table 6. The toryx charge e is proportional to the toryx vorticity $\tilde{V}$ with an opposite sign, the toryx inertial mass m_i is proportional to the toryx vorticity $\tilde{V}$, and the toryx gravitational mass m_g is proportional to the absolute value of the toryx vorticity $\tilde{V}$.

Relative toryx charge	$\frac{e}{e_0} = -\tilde{V}$	(31)
Relative toryx inertial mass	$\frac{m_i}{m_0} = \tilde{V}$	(32)
Relative toryx gravitational mass	$\frac{m_g}{m_0} = \lvert\tilde{V}\rvert$	(33)

Table 6. Equations for toryx relative charge and mass

Relative toryx charge	$\frac{e}{e_0} = -\sqrt{1-\beta_1^2}$	(34)
Relative toryx inertial mass	$\frac{m_i}{m_0} = \sqrt{1-\beta_1^2}$	(35)
Relative toryx gravitational mass	$\frac{m_g}{m_0} = \lvert\sqrt{1-\beta_1^2}\rvert$	(36)

Table 7. Relativistic equations for toryx relative charge and mass

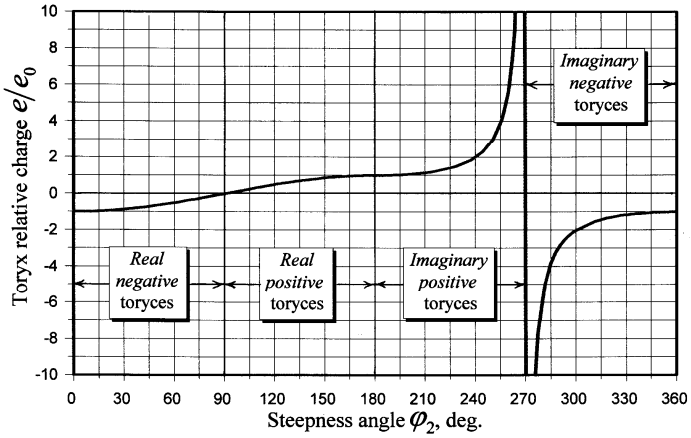

Fig. 25. Toryx relative charge e/e_0 as a function of the steepness angle of trailing string φ_2

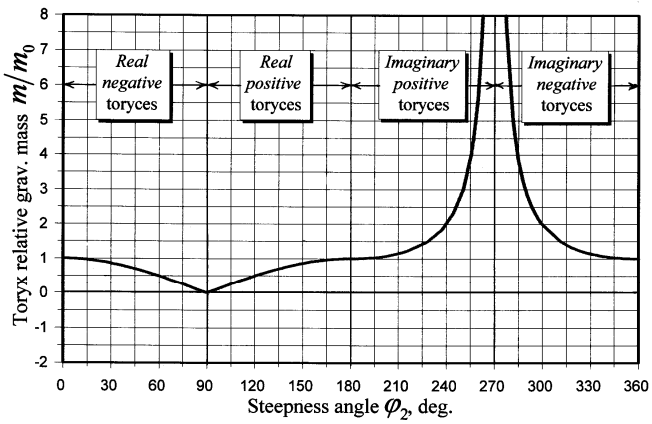

Fig. 26. Toryx relative gravitational mass m/m_0 as a function of the steepness angle of trailing string φ_2

Table 7 shows relativistic equations for the toryx relative charge and mass as a function of the relative velocity of leading string β_1. Notably, the relativistic effects are opposite for real and imaginary toryces. Since in the real toryces $\beta_1^2 > 0$, the magnitudes of the toryx charge and mass decrease when the relative velocity of leading string β_1 increases. Conversely, since in the imaginary toryces $\beta_1^2 < 0$, the magnitudes of the toryx charge and mass increase when the relative velocity of leading string β_1 increases.

The values of the toryx charge and masses are expressed in the circular diagrams of Figs. 27 – 29 as a function of the steepness angle of trailing string φ_2. These diagrams illustrate a specific symmetry between these parameters in the four types of toryces: the real negative toryces, the real positive toryces, the imaginary positive toryces and the imaginary negative toryces.

The toryx relative total energy E_{tr} is equal to the sum of its relative kinetic and potential energies. It is given by the equation:

$$E_{tr} = \frac{E_t}{m_0 c^2} = -\frac{(b_1 - 1)(2b_1 - 1)}{2b_1^3} \tag{37}$$

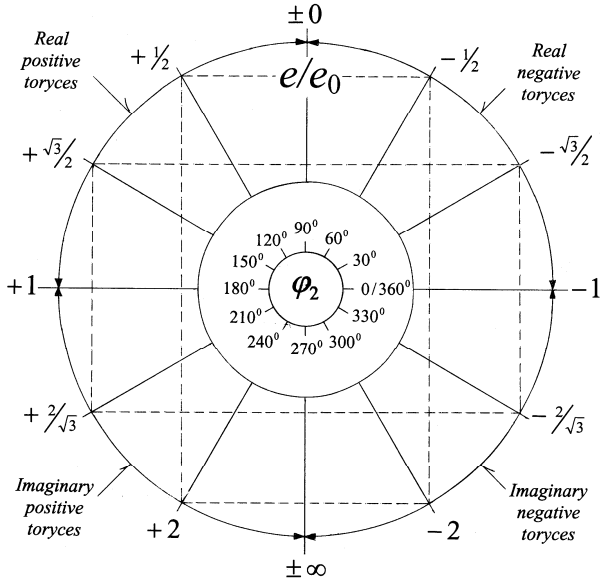

Fig. 27. Toryx relative charge e/e_0 as a function of the steepness angle of trailing string φ_2

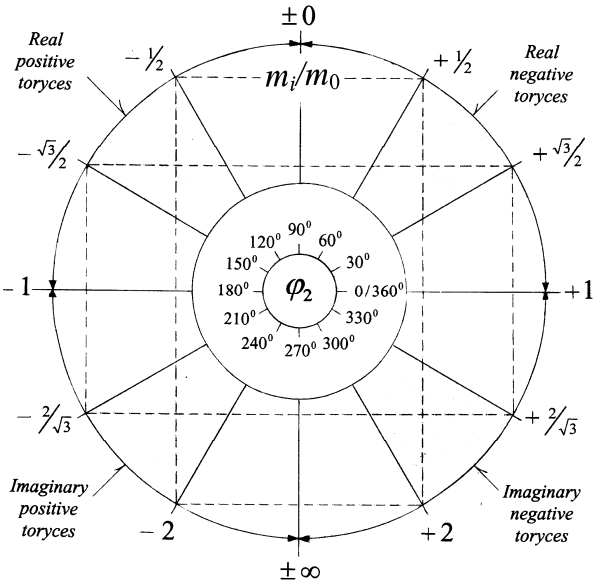

Fig. 28. Toryx relative inertial m_i/m_0 as a function of the steepness angle of trailing string φ_2

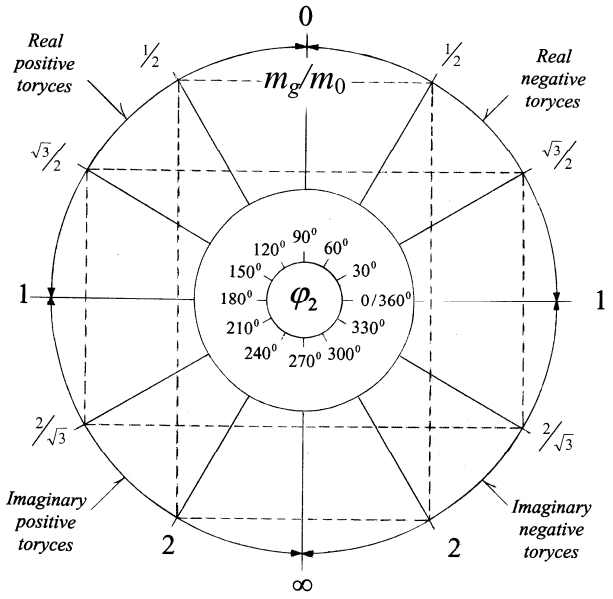

Fig. 29. Toryx relative gravitational m_g/m_0 as a function of the steepness angle of trailing string φ_2

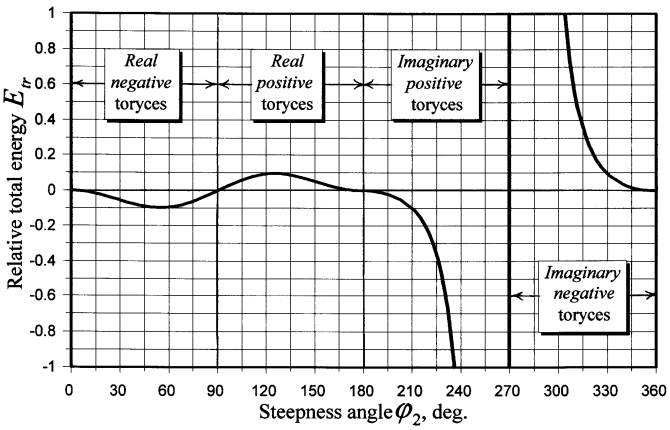

Fig. 30. Toryx relative total energy E_{tr} as a function of the steepness angle of trailing string φ_2

Figure 30 shows a trend of the toryx relative total energy E_{tr} as a function of the steepness angle of trailing string φ_2.

6.3. Toryx Mechanical and Magnetic Properties

Table 8 shows equations for the two toryx mechanical properties, the toryx relative density ρ_r and the toryx relative Young's modulus of elasticity Y_r. The magnetic properties are presented by the two toryx relative magnetic moments, Bohr and nuclear.

The relative Bohr magnetic moment μ/μ_B is expressed relative to the Bohr magneton μ_B given by the equation:

$$\mu_B = \frac{e_0^3}{8\pi\alpha\varepsilon_0 m_0 c} \tag{38}$$

The toryx relative nuclear magnetic moment μ/μ_n is expressed relative to the nuclear magneton μ_n given by the equation:

$$\mu_n = \frac{e_0^3}{8\pi\alpha\varepsilon_0 m_p c} \tag{39}$$

Thus, $\mu_n/\mu_B = m_0/\mu_p$. In Eqs. (38) and (39):

a = fine composition constant
m_p = proton mass.

Toryx relative density	$\rho_r = \rho\frac{2\pi^2 r_i^3}{m_0} = \frac{1}{b_1\lvert b_1^2 - b_1\rvert}$	(40)
Toryx relative Young's modulus of elasticity	$Y_r = Y\frac{2\pi^2 r_i^3}{m_0 c^2} = \frac{2b_1 - 1}{b_1^3\lvert b_1^2 - b_1\rvert}$	(41)
Real toryx relative Bohr magnetic moment	$\mu / \mu_B = \pm\frac{Z\alpha(b_1 - 1)\sqrt{2b_1 - 1}}{2b_1}$	(42)
Imaginary toryx relative Bohr magnetic moment	$\mu / \mu_B = \pm\frac{iZ\alpha(b_1 - 1)\sqrt{2b_1 - 1}}{2b_1}$	(43)

Table 8. Equations for toryx relative mechanical and magnetic properties

Figures 31 – 33 show the trends of the toryx mechanical and magnetic parameters as a function of the steepness angle of trailing string φ_2. The relative Bohr magnetic moment is given for the case when the atomic number $Z = 1$.

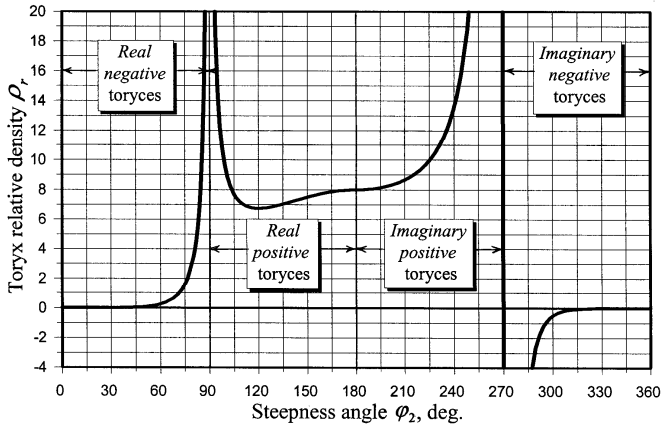

Fig. 31. Toryx relative density ρ_r as a function of the steepness angle of trailing string φ_2.

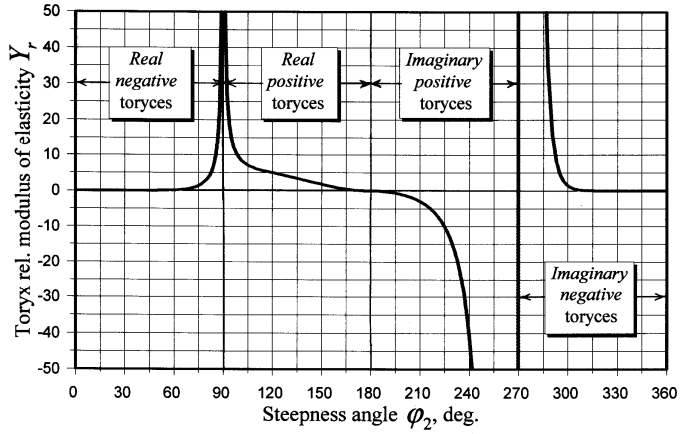

Fig. 32. Toryx relative Young's modulus of elesticity Y_r as a function of the steepness angle of trailing string φ_2

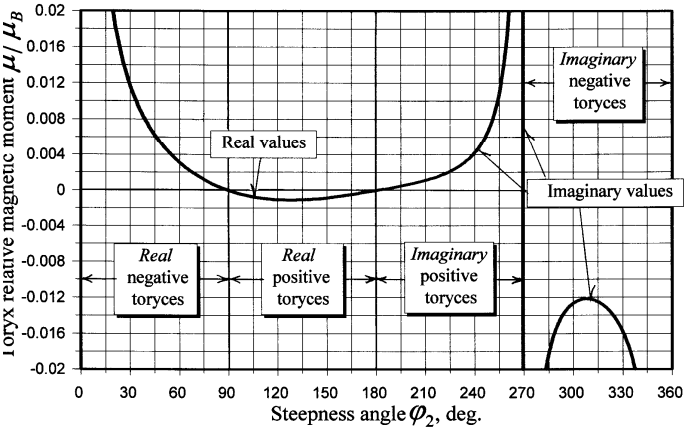

Fig. 33. Toryx relative Bohr magnetic moment μ/μ_B as a function of the steepness angle of trailing string φ_2

7. Classification of Toryces and Trons

7.1. Toryces

In Sections 3 – 6 we described four main groups of toryces, including:

- Real negative (outverted) toryces
- Real positive (inverted) toryces
- Imaginary positive (inverted) toryces
- Imaginary negative (outverted) toryces

As shown in Table 9 and Fig. 34, each main group of real toryces is divided into two sub-groups of toryces, and each main group of imaginary toryces is divided into three sub-groups of toryces. So, in total we consider ten types of toryces.

We use capital Latin letters for the symbols of toryces. The top superscripts indicate the sign (and value wherever possible) of their charges. A "smiling cup" over the toryx symbols identifies the imaginary toryces.

Main groups of toryces		**Sub-groups of toryces**		
Name	Range of φ_2	Symbol	Range of b_1	
Real negative toryces	$+0 < \phi_2 < \frac{1}{2}\pi$	E^-	$+\infty$	2.0
		A^-	2.0	1.0
Real positive toryces	$\frac{1}{2}\pi < \phi_2 < \pi$	A^+	1.0	$\frac{2}{3}$
		E^+	$\frac{2}{3}$	$\frac{1}{2}$
Imaginary positive toryces	$\pi < \phi_2 < \frac{3}{2}\pi$	$\breve{E}^-$	$\frac{1}{2}$	$\frac{2}{5}$
		$\breve{A}^+$	$\frac{2}{5}$	$\frac{1}{3}$
		$\breve{Z}^+$	$\frac{1}{3}$	+0
Imaginary negative toryces	$\frac{3}{2}\pi < \phi_2 < 2\pi$	$\breve{Z}^-$	-0	-1.0
		$\breve{A}^-$	-1.0	-2.0
		$\breve{E}^-$	-2.0	$-\infty$

Table 9. Classification of toryces

The real negative toryces are divided into the real negative a-toryces A^- and the real negative e-toryces E^-. The real positive toryces are divided into the real positive a-toryces A^+ and the real positive e-toryces E^+. The imaginary positive toryces are divided into the imaginary positive e-toryces $\breve{E}^+$, the imaginary positive a-toryces $\breve{A}^+$, and the imaginary positive z-toryces $\breve{Z}^+$. The imaginary negative toryces are divided into the imaginary negative z-toryces $\breve{Z}^-$, the imaginary negative a-toryces $\breve{A}^-$ and the imaginary negative e-toryces $\breve{E}^-$.

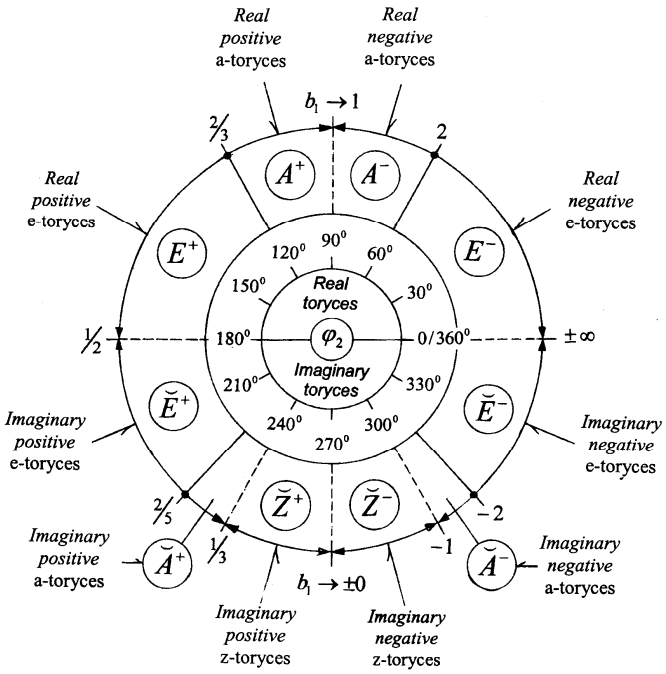

Fig. 34. Ten types of toryces

7.2. Trons

Trons are the elementary particles made up of matched toryces. Consider a couple of toryces with the relative charges $\varepsilon' = e'/e_0$ and $\varepsilon'' = e''/e_0$. In the matched toryces the algebraic average of their relative charges ε' and ε'' is equal to a certain value called the *tron relative charge* ε_t.

$$\varepsilon_t = \frac{e_t}{e_0} = \frac{\varepsilon' + \varepsilon''}{2} \tag{44}$$

The relative radii of leading strings of matched toryces b_1' and b_1'' are related to one another by the equation:

$$b_1'' = \frac{b_1'}{2b_1'(\varepsilon_t + 1) - 1} \tag{45}$$

We use the lower-case Latin letters for the symbols of trons. There are two main types of trons, reality-polarized and charge-polarized (Fig. 35).

Charge-polarized trons. The constituent toryces of charge-polarized trons have opposite charges. Both these toryces can be either real or imaginary.

Reality-polarized trons. In the reality-polarized trons, one of the toryces is real while the other one is imaginary. The total charge of these trons can be either negative or positive.

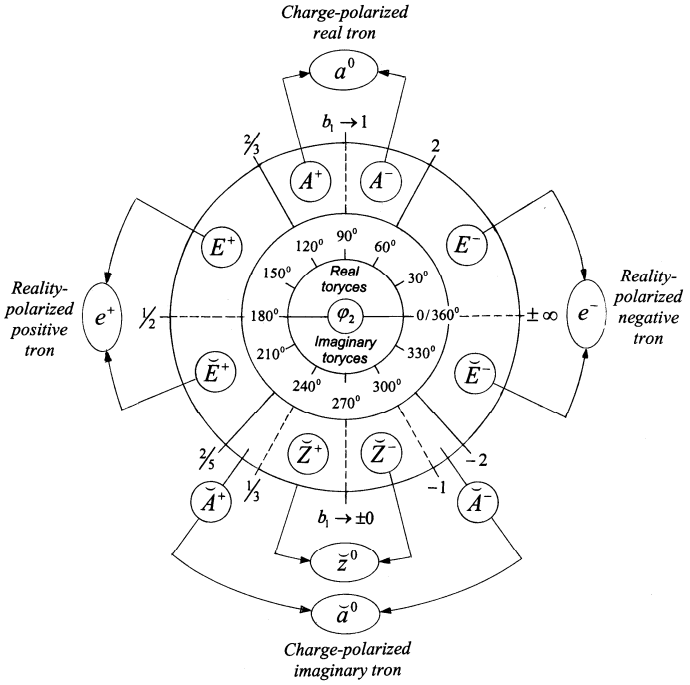

Fig. 35. Types of trons

Any physical property of a tron is equal to an algebraic average of the respective properties of its constituent toryces.

8. Quantum Energy States of Toryces

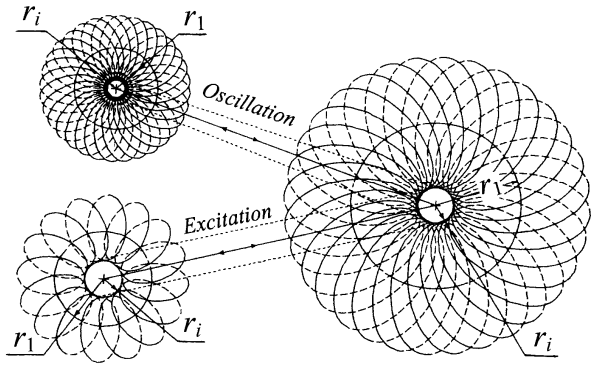

Fig. 36. Two types of quantum energy states of toryces: excitation and oscillation

Toryces change their energy states in quantum steps by oscillation and excitation (Fig. 36). During the excitation of a toryx, the radius of leading string r_1 changes, while the radius of real inversion string r_i remains constant. During the oscillation of a toryx, the radius of real inversion string r_i changes proportionally with the radius of leading string r_1.

8.1. Oscillation Quantum States of Toryces

During the oscillation of a toryx its real inversion string r_i is assumed to be changing inversely proportional to the *toryx oscillation factor* Q_p defined by the equation below.

$$Q_0 = 1$$
$$Q_p = 3\big(2\alpha(p-1)\big)^{1-p} = \frac{r_{i0}}{r_{ip}} \tag{46}$$

where p = 1, 2,…toryx oscillation quantum state.

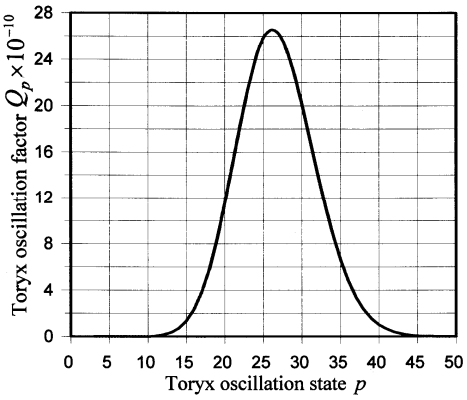

Fig. 37. Toryx oscillation factor Q_p as a function of the toryx oscillation state p.

A plot of Eq. (46) appears as a bell-type curve (Fig. 37). Initially, the toryx oscillation factor increases with the increase of the toryx oscillation quantum state p. At $p = p_m$, Q_p reaches its maximum value Q_{pm}:

$$p_m = 1 + \frac{1}{2\alpha e} = 26.206363 \tag{47}$$

$$Q_{pm} = 3e^{1/2\alpha e} = 2.655252 \times 10^{11} \tag{48}$$

where e is the base of natural logarithms.

The ratios of the toryx parameters at the oscillation quantum states $p > 0$ and $p = 0$ are given by the equation.

$$Q_p = \frac{r_{i0}}{r_{ip}} = \frac{f_{ip}}{f_{i0}} = \frac{m_{ip}}{m_{i0}} = \frac{m_{gp}}{m_{g0}} = \frac{\mu_0}{\mu_p} \tag{49}$$

8.2. Excitation Quantum States of Toryces

Table 10 presents the equations for the excitation quantum states of toryces listed in Table 9. The relative radii of leading strings of these toryces b_1 are assumed to be a function of the *quantization parameter z*:

$$z = n + 2(n/\alpha)^m \tag{50}$$

where

m = 0, 1,…toryx exponential excitation quantum state

n = 0, 1,…toryx linear excitation quantum state

The subscripts of the symbols of the toryces shown in Table 10 indicate the excitation quantum states m and n and also the

oscillation quantum state p. The quantization equations listed in Table 10 are based on the basic equation applied to the real negative toryx $E^{-}_{m,n,p}$:

$$b_1(E^{-}_{m,n,p}) = z \tag{51}$$

Toryx	**Range of b_1**		**Equation**	
$E^{-}_{m,n,p}$	+∞	2.0	$b_1 = z$	(51)
$A^{-}_{m,n,p}$	2.0	1.0	$b_1 = \frac{z}{z-1}$	(52)
$A^{+}_{m,n,p}$	1.0	⅔	$b_1 = \frac{z}{z+1}$	(53)
$E^{+}_{m,n,p}$	⅔	½	$b_1 = \frac{z}{2z-1}$	(54)
$\breve{E}^{+}_{m,n,p}$	½	⅖	$b_1 = \frac{z}{2z+1}$	(55)
$\breve{A}^{+}_{m,n,p}$	⅖	⅓	$b_1 = \frac{z}{3z-1}$	(56)
$Z^{+}_{m,n,N}$	⅓	+0	$b_1 = \frac{1}{z}$	(57)
$Z^{-}_{m,n,N}$	-0	-1.0	$b_1 = \frac{1}{2-z}$	(58)
$\breve{A}^{-}_{m,n,p}$	-1.0	-2.0	$b_1 = -\frac{u}{u-1}$	(59)
$\breve{E}^{-}_{m,n,p}$	-2.0	-∞	$b_1 = -u$	(60)

Table 10. Excitation quantum states of toryces forming the trons with the relative charges expressed by integers

The remaining equations (52) – (60) shown in Table 10 are derived from Eqs. (45) and (51), assuming that the toryces form the trons with the relative charges either neutral or expressed by the whole numbers (+1 and -1).

The excitation toryces are further divided into harmonic and exponential based on their quantization states (Table 11). The frequencies of trailing strings of harmonic toryces relate to one another by simple harmonic ratios, explaining their name.

Toryx	m	n	p
Harmonic	0	0, 1,…	0, 1,…
Exponential	1,2,…	0, 1,…	0, 1,…

Table 11. Quantum states of harmonic and exponential toryces

9. Formation of Elementary Particles

We will show below several examples of compositions and calculated parameters of elementary particles.

9.1. Electrons and positrons

The electrons $e^{-1}_{m,n,p}$ and the positrons $e^{+1}_{m,n,p}$ are respectively the reality-polarized negative and positive e-trons (Fig. 38).

The electrons $e^{-1}_{m,n,p}$ are formed from the real negative e-toryces $E^{-1}_{m,n,p}$ and the imaginary negative e-toryces $\breve{E}^{-1}_{m,n,p}$. The positrons $e^{+1}_{m,n,p}$ are formed from the real positive e-toryces $E^{+1}_{m,n,p}$ and the imaginary positive e-toryces $\breve{E}^{+1}_{m,n,p}$.

$$e^{-1}_{m,n,p} = E^{-}_{m,n,p} + \breve{E}^{-}_{m,n,p} \tag{61}$$

$$e^{+1}_{m,n,p} = E^{+}_{m,n,p} + \breve{E}^{+}_{m,n,p} \tag{62}$$

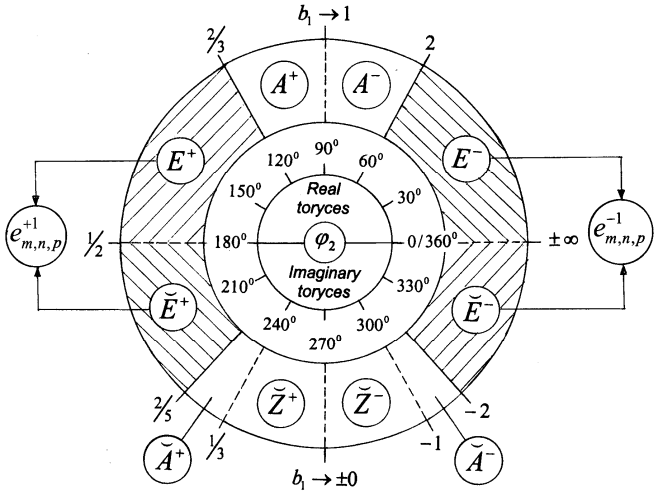

Fig. 38. Formation of electrons $e^{-1}_{m,n,p}$ and positrons $e^{+1}_{m,n,p}$.

Tables 12 - 15 show the compositions and properties of harmonic and exponential electrons and positrons.

Harmonic e-trons			**Toryces**	
Name	μ / μ_n	m_g MeV/c²	Symbol	b_1
$e^{-1}_{0,0,0}$	± 14.13642820	0.51099891	$E^{-1/4}_{0,0,0}$	2.0
			$\breve{E}^{-3/4}_{0,0,0}$	-2.0
$e^{-1}_{0,1,0}$	± 16.81038698	0.51099891	$E^{-1/3}_{0,1,0}$	3.0
			$\breve{E}^{-2/3}_{0,1,0}$	-3.0
$e^{-1}_{0,2,0}$	± 19.20859341	0.51099891	$E^{-3/8}_{0,2,0}$	4.0
			$\breve{E}^{-5/8}_{0,2,0}$	-4.0

Table 12. Reality-polarized negative harmonic electrons (m = 0, p = 0)

Harmonic e-trons			**Toryces**	
Name	μ/μ_N	m_g MeV/c²	Symbol	b_1
$e^{+1}_{0,0,0}$	± 3.214083	0.51099891	$E^{+1/4}_{0,0,0}$	⅔
			$\breve{E}^{+3/4}_{0,0,0}$	⅖
$e^{+1}_{0,1,0}$	± 2.686828	0.51099891	$E^{+1/3}_{0,1,0}$	⅗
			$\breve{E}^{+2/3}_{0,1,0}$	⅜
$e^{+1}_{0,2,0}$	± 2.345303	0.51099891	$E^{+3/8}_{0,2,0}$	⅘
			$\breve{E}^{+5/8}_{0,2,0}$	⅘

Table 13. Reality-polarized positive harmonic positrons (m = 0, p = 0)

Exponential e-trons			Toryces	
Name	μ/μ_B	m_g MeV/c²	Symbol	b_1
$e^{-1}_{2,0,0}$	± 0.0	∞	$E^{-}_{2,0,0}$	+0
			$\breve{E}^{-}_{2,0,0}$	–0
$e^{-1}_{2,1,0}$	± 1.00001331	0.51099891	$E^{-}_{2,1,0}$	37558.7
			$\breve{E}^{-}_{2,1,0}$	-37558.7
$e^{-1}_{2,2,0}$	± 2.00001331	0.51099891	$E^{-}_{2,2,0}$	150232.9
			$\breve{E}^{-}_{2,2,0}$	-150232.9

Table 14. Reality-polarized negative exponential electrons (m = 2, p = 0)

Exponential e-trons			Toryces	
Name	μ/μ_n	m_g MeV/c²	Symbol	b_1
$e^{+1}_{2,0,0}$	± 0.0	∞	$E^{+}_{2,0,0}$	–0
			$\breve{E}^{+}_{2,0,0}$	+0
$e^{+1}_{2,1,0}$	± 0.02444	0.51099891	$E^{+}_{2,1,0}$	0.50000666
			$\breve{E}^{+}_{2,1,0}$	0.49999334
$e^{+1}_{2,2,0}$	± 0.01222	0.51099891	$E^{+}_{2,2,0}$	0.50000166
			$\breve{E}^{+}_{2,2,0}$	0.49999834

Table 15. Reality-polarized positive exponential positrons (m = 2, p = 0)

Figure 39 shows the cross-sections of the harmonic electron $e^{-1}_{0,0,0}$ and positron $e^{+1}_{0,0,0}$ at the lowest quantum states m = 0, n = 0 and p = 0.

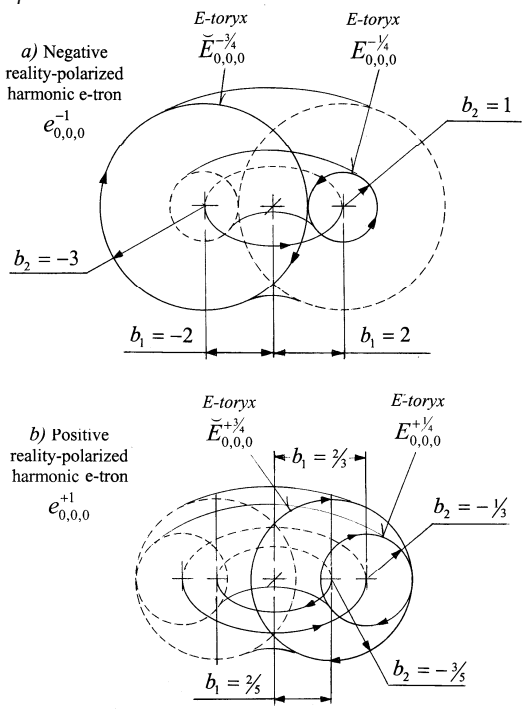

Fig. 39. Cross-sections of: a) the harmonic electron $e^{-1}_{0,0,0}$ and b) the harmonic positron $e^{+1}_{0,0,0}$

9.2. Neutral Aetherons

The neutral real aetherons $a^0_{m,n,p}$ and the neutral imaginary aetherons $\breve{a}^0_{m,n,p}$ are respectively the charge-polarized real and imaginary a-trons (Fig. 40). The real aetherons $a^0_{m,n,p}$ are formed from the real negative a-toryces $A^-_{m,n,p}$ and the real positive a-toryces $A^+_{m,n,p}$. The imaginary aetherons $\breve{a}^0_{m,n,p}$ are formed from the imaginary negative a-toryces $\breve{A}^-_{m,n,p}$ and the imaginary positive a-toryces $\breve{A}^+_{m,n,p}$.

$$a^0_{m,n,p} = A^-_{m,n,p} + A^+_{m,n,p} \tag{63}$$

$$\breve{a}^0_{m,n,p} = \breve{A}^-_{m,n,p} + \breve{A}^+_{m,n,p} \tag{64}$$

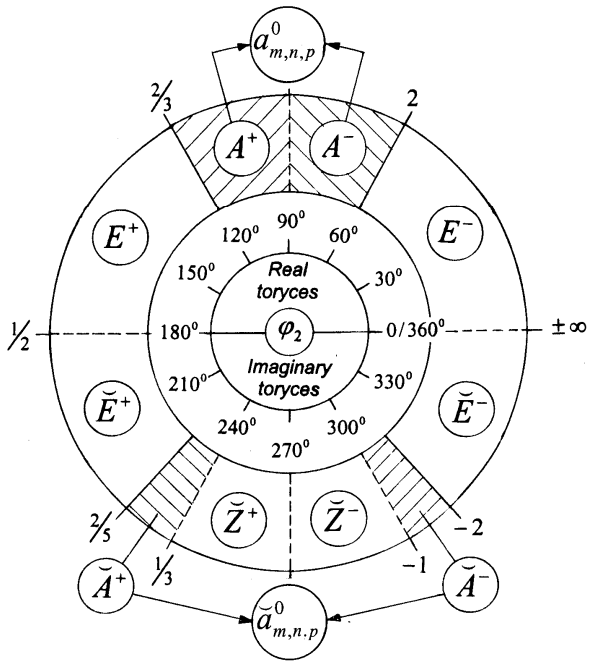

Fig. 40. Formation of the real aetherons $a^0_{m,n,p}$ and the imaginary aetherons $\breve{a}^0_{m,n,p}$

Tables 16 - 19 show the compositions and properties of harmonic and exponential aetherons.

Harmonic a-trons			Toryces	
Name	μ/μ_n	m_g MeV/c²	Symbol	b_1
$a^0_{0,0,0}$	± 1.93398680	0.25549946	$A^{-1/4}_{0,0,0}$	2.0
			$A^{+1/4}_{0,0,0}$	2/3
$a^0_{0,1,0}$	± 0.78954680	0.17033297	$A^{-1/6}_{0,1,0}$	3/2
			$A^{+1/6}_{0,1,0}$	3/4
$a^0_{0,2,0}$	± 0.43245260	0.12774973	$A^{-1/8}_{0,2,0}$	4/3
			$A^{+1/8}_{0,2,0}$	4/5

Table 16. Charge-polarized real harmonic aetherons (m = 0, p = 0)

Harmonic a-trons			Toryces	
Name	μ/μ_n	m_g MeV/c²	Symbol	b_1
$\breve{a}^0_{0,0,0}$	± 8.98835840	0.76649837	$\breve{A}^{-3/4}_{0,0,0}$	- 2.0
			$\breve{A}^{+3/4}_{0,0,0}$	$2/5$
$\breve{a}^0_{0,1,0}$	± 8.37440849	0.85166485	$\breve{A}^{-5/6}_{0,1,0}$	$-3/2$
			$\breve{A}^{+5/6}_{0,1,0}$	$3/8$
$\breve{a}^0_{0,2,0}$	± 8.16366544	0.89224809	$\breve{A}^{-7/8}_{0,2,0}$	$-4/3$
			$\breve{A}^{+7/8}_{0,2,0}$	$4/11$

Table 17. Charge-polarized imaginary harmonic aetherons (m=0, p=0)

Exponential a-trons			Toryces	
Name	μ/μ_n	m_g MeV/c²	Symbol	b_1
$a^0_{2,0,0}$	±0.0	∞	$A^-_{2,0,0}$	–0
			$A^+_{2,0,0}$	+0
$a^0_{2,1,0}$	$\pm 4.75\times10^{-9}$	0.0000136	$A^-_{2,1,0}$	1.0000266
			$A^+_{2,1,0}$	0.9999734
$a^0_{2,2,0}$	$\pm 2.97\times10^{-10}$	0.0000034	$A^-_{2,2,0}$	1.0000067
			$A^+_{2,2,0}$	0.9999933

Table 18. Charge-polarized real exponential aetherons (m = 2, p = 0)

Exponential a-trons			Toryces	
Name	μ/μ_n	m_g MeV/c²	Symbol	b_1
$\breve{a}^0_{2,0,0}$	±0.0	∞	$\breve{A}^-_{2,0,0}$	+0
			$\breve{A}^+_{2,0,0}$	–0
$\breve{a}^0_{2,1,0}$	± 7.735981	1.02198421	$\breve{A}^-_{2,1,0}$	-1.00002663
			$\breve{A}^+_{2,1,0}$	0.33333629
$\breve{a}^0_{2,2,0}$	± 7.735956	1.02198421	$\breve{A}^-_{2,2,0}$	-1.00000666
			$\breve{A}^+_{2,2,0}$	0.33333407

Table 19. Charge-polarized imaginary exponential aetherons (m=2, p=0)

Figure 41 shows the cross-sections of the real harmonic aetheron $a^0_{0,0,0}$ at the lowest quantum states m = 0, n = 0 and p = 0.

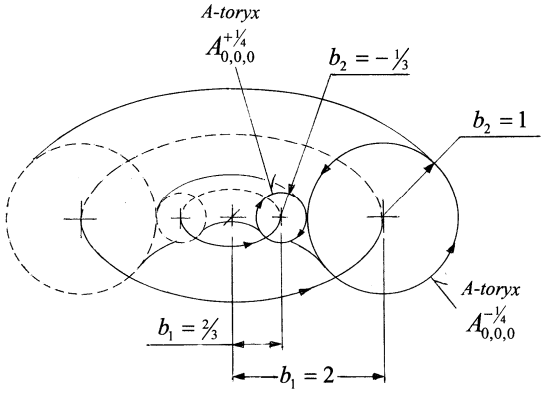

Fig. 41. Cross-sections of the real harmonic aetheron $a^0_{0,0,0}$

9.3. Zerotrons

The neutral imaginary zerotrons $\breve{z}^0_{m,n,p}$ are the charge-polarized imaginary z-trons (Fig. 42). They are formed from the imaginary negative z-toryces $\breve{Z}^-_{m,n,p}$ and the imaginary positive z-toryces $\breve{Z}^+_{m,n,p}$.

$$\breve{z}^0_{m,n,p} = \breve{Z}^-_{m,n,p} + \breve{Z}^+_{m,n,p} \tag{65}$$

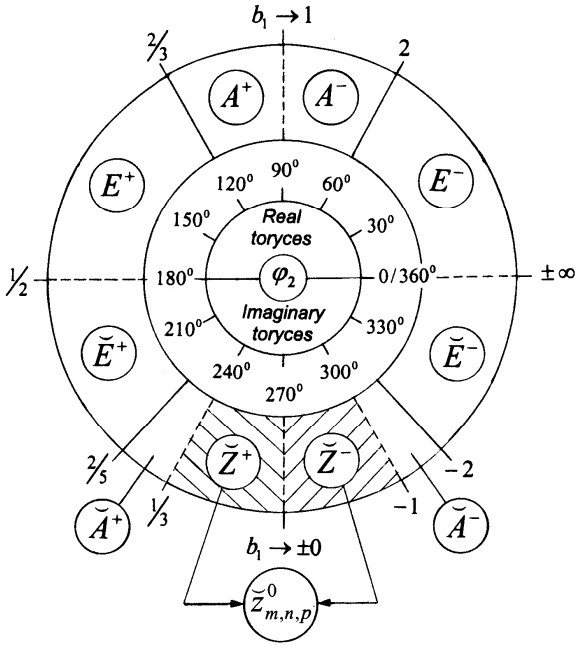

Fig. 42. Formation of the imaginary zerotrons $\breve{z}^0_{m,n,p}$

Table 20 shows the compositions and properties of neutral exponential zerotrons.

Exponential z-trons			Toryces	
Name	μ/μ_n	m_g MeV/c²	Symb.	b_1
$\breve{z}^0_{1,0,0}$	± ∞	0.51099891	$\breve{Z}^-_{1,0,0}$	+∞
			$\breve{Z}^+_{1,0,0}$	0.5
$\breve{z}^0_{1,1,0}$	± 6.699571	140.050493	$\breve{Z}^-_{1,1,0}$	-0.00366204
			$\breve{Z}^+_{1,1,0}$	0.00363541
$\breve{z}^0_{1,2,0}$	± 6.699538	280.611985	$\breve{Z}^-_{1,2,0}$	-0.00182434
			$\breve{Z}^+_{1,2,0}$	0.00181771
$\breve{z}^0_{1,3,0}$	± 6.699532	421.173476	$\breve{Z}^-_{1,3,0}$	-0.00121475
			$\breve{Z}^+_{1,3,0}$	0.00121180

Table 20. Charge-polarized exponential zerotrons (m = 1, p = 0)

9.4. Leptons

Leptons are the oscillated electrons and positrons. Table 21 shows the compositions and properties of leptons for the case when m = 2 and n = 1. This would correspond to the relative radii of leading strings of real toryces b_1 = 37557.73 and imaginary toryces b_1 = -37557.73. The calculated lepton magnetic moment for all leptons μ/μ_L = -0.9999999895.

p	Q_p	Toryx	Lepton	m_g MeV/c²
0	1.00	$E^-_{2,1,0}$ / $\breve{E}^-_{2,1,0}$	Electron $e^-_{2,1,0}$	0.51099892
1	3.00	$E^-_{2,1,1}$ / $\breve{E}^-_{2,1,1}$	3electron $e^-_{2,1,1}$	1.53299675
2	205.554	$E^-_{2,1,2}$ / $\breve{E}^-_{2,1,2}$	Muon $e^-_{2,1,2}$	105.037872
3	3521.037	$E^-_{2,1,3}$ / $\breve{E}^-_{2,1,3}$	Tau $e^-_{2,1,3}$	1799.246
4	35741.40	$E^-_{2,1,4}$ / $\breve{E}^-_{2,1,4}$	X-lepton $e^-_{2,1,4}$	18263.82

Table 21. Compositions and physical properties of leptons (m = 2, n = 1)

10. Creation of Stable Elementary Particles

There are two conditions for the creation of stable elementary particles. Firstly, to create a stable elementary particle its constituent toryces must comply with the *toryx creation principle* that is similar to the Heisenberg's uncertainty principle. Secondly, for the created elementary particle to become stable it must be continuously recreated again and again. This occurs by following the *universal conservation law*.

Toryx creation principle. According to the toryx creation principle a product of the total toryx energy E_t by the cycle time of its trailing string t_1 should not be greater than h/π:

$$E_t \cdot t_1 \le \frac{h}{\pi} \tag{66}$$

The solution of Eq. (66) reduces to the form:

$$\frac{(b_1 - 1)\sqrt{2b_1 - 1}}{b_1} \le \frac{8}{\pi Z \alpha} \tag{67}$$

It follows from Eq. (67) that when Z = 1, its condition is met for the toryces within the following ranges of their relative radii of leading strings:

$$\begin{aligned} -0.002882194 \le b_1 \le -60888.79865 \\ 0.002849345 \le b_1 \le \quad 60888.79865 \end{aligned} \tag{68}$$

The universal conservation law. The life of the created elementary particles will be sustained when the total energy of its constituent polarized toryces approaches to infinility. In case of a complex particle made up of several elementary particles, the complex particle will be stable if the total energy of its constituent elementary particles approaches to infinility.

11. The Universal Law of Motion

Three fundamental spacetime equations of the toryx shown in Table 1 yield Equation (5) describing a unique relationship between the relative velocity of leading string β_1 and the relative radius of leading string b_1. We call this relationship *the universal law of motion.* Table 22 compares Eq. (5) with the two known laws of motion: the classical law of motion and the relativistic law of motion. The comparison is made in an application to an atomic electron.

The classical law of motion is commonly derived by considering the equilibrium of an attraction force between the two polarized particles and a repulsion centrifugal force applied to the orbiting particle. The relativistic law of motion further refines the classical law of motion by considering a well-known relativistic dependence of the particle mass on its velocity used in the special theory of relativity. In our calculations, we assumed that the radius of the real inversion string r_i is described by Eq. (29).

Universal law of motion	Classical law of motion	Relativistic law of motion
$\beta_1 = \frac{\sqrt{2b_1 - 1}}{b_1}$	$\beta_1 = \sqrt{\frac{2}{b_1}}$	$\beta_1 = \frac{\sqrt{2}}{b_1}\left(\sqrt{b_1^2 + 1} - 1\right)^{1/2}$

Table 22. Comparison of equations for three laws of motion

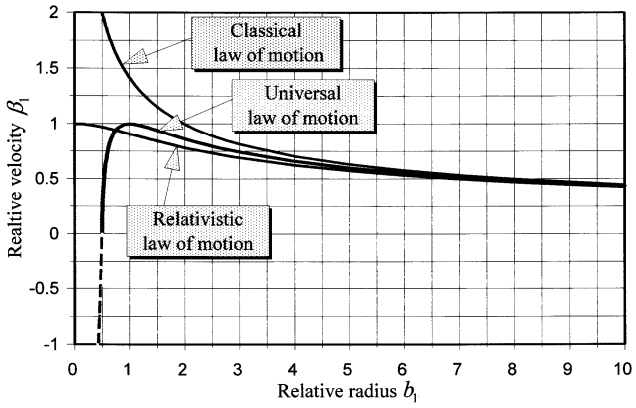

Fig. 43. Comparison of plots of equations for three laws of motion

It follows from the plots of the equations shown in Table 22 (Fig. 43) that all three laws yield very close values of the relative velocity β_1 when the relative radius b_1 is greater than 10. Notably, as shown in Table 14, for the atomic electrons at the ground quantum level n = 1 the relative radius b_1= 37558.7. Thus, for this radius all three laws would predict practically the same values. The difference between the predictions by these three laws becomes significant when the relative radius b_1 are less than 5. This range of b_1 corresponds to the toryces forming nuclear e-trons, and also a-trons and z-trons.

Conclusion

1. According to the Three-Dimensional Spiral String Theory (3D-SST), at the elementary level, the universe is made up of polarized spacetime spiral-string entities called *toryces*.
2. The toryx is a spacetime spiral string element containing a circular leading string and a toroidal trailing string propagating with the velocity of light synchronously with the propagation of leading string.
3. All spacetime properties of the toryces can be derived from its three fundamental equations. The analysis of the toryx spacetime equations reveals its several unique properties, including:

- The toryx exists in four principal polarized forms associated with the inversion of its vorticity and reality.
- There is a unique symmetry between the spacetime properties of the toryces that belong to the different polarized forms.
- The velocity of propagation of the toryx leading string follows a newly-discovered universal law of motion, and both the classical law of motion and the relativistic law of motion can be considered as its particular cases.
- The math description of the toryx spacetime requires a modification of conventional math that includes: (a) a replacement of a conventional zero with the infinility that is the inverse of infinity, (b) the modification of a conventional trigonometry and (c) a new presentation of a number line.

4. Physical properties of the toryces are directly related to its spacetime properties.
5. Toryces change their energy states in quantum steps by oscillation and excitation according to the proposed quantization equations. Both processes involve absorption and release of energy in the form of the prime elements of radiation particles called helyces.
6. The toryces create elementary particles by the unification of properly matched polarized toryces. The theory allows for the existence of particles with both whole and fractional charges. There are four principal elementary particles:
   - Negative e-trons that form electrons
   - Positive e-trons that form positrons
   - Neutral a-trons that form the particles of aether and quantum vacuum
   - Neutral z-trons that form heavy particles and a singularity.
7. The creation of the elementary particles is governed by the toryx creation principle that is similar to the Heisenberg's uncertainty principle and the proposed universal conservation law.

References

[1] V.B. Ginzburg, "The Unification of Forces," Proceedings of the Natural Philosophy Alliance, Vol. 4, No. 1, 2007.

[2] V.B. Ginzburg, **Prime Elements of Ordinary Matter, Dark Matter & Dark Energy – Beyond Standard Model & String Theory**, The Second Revised Edition (Universal Publishers, Boca Raton, Florida 2007).

[3] V.B. Ginzburg, **Prime Elements of Ordinary Matter, Dark Matter & Dark Energy – Beyond Standard Model & String Theory**, The Second Revised Edition, hard cover (www.lulu.com 2007).

[4] V.B. Ginzburg, **Prime Elements of Ordinary Matter, Dark Matter & Dark Energy** (Helicola Press, Pittsburgh, PA, 2006).

[5] V.B. Ginzburg, "The Relativistic Torus and Helix as the Prime Elements of Nature," Proceedings of the Natural Philosophy Alliance, Vol. 1, No. 1, Spring 2004.

[6] V.B. Ginzburg, "Unified Spiral Field Theory – A Quiet Revolution in Physics," *VIA-Vision in Action*, Vol. 2, No. 1 & 2, 2004.

[7] V.B. Ginzburg, **The Unification of Strong, Gravitational & Electric Forces** (Helicola Press, Pittsburgh, PA, 2003).

[8] V.B. Ginzburg, "Electric Nature of Strong Interactions," Journal of New Energy, Vol. 7, No. 1, 2003.

[9] V.B. Ginzburg, "Dynamic Aether," *Journal of New Energy*, Vol. 6, No. 1, 2001.

[10] V.B. Ginzburg, "Nuclear Implosion," *Journal of New Energy*, Vol. 3, No. 4, 1999.

[11] V.B. Ginzburg, **Unified Spiral Field and Matter - A Story of a Great Discovery**, Helicola Press, Pittsburgh, PA, 1999.

[12] V.B. Ginzburg, "Double Helical and Double Toroidal Spiral Fields," *Speculations in Science and Technology*, Vol. 22, 1998.

[13] V.B. Ginzburg, "Structure of Atoms and Fields," *Speculations in Science and Technology*, Vol. 20, 1997.

[15] V.B. Ginzburg, **Spiral Grain of the Universe - In Search of the Archimedes File**, University Editions, Inc., Huntington, WV, 1996.

[16] V.B. Ginzburg, "Toroidal Spiral Field Theory," *Speculations in Science and Technology*, Vol. 19, 1996.